A Finite Element Method for solving Maxwell's equations: first application in dispersed materials.

Journées d'études en rayonnement thermique, 2018

Tom Mathew, Dr. Yann Favennec, Dr. Benoit Rousseau

Laboratoire de Thermique et Énergie de Nantes

UNIVERSITÉ DE NANTES

POLYTECH NANTES

Gif-sur-Yvette, France ◆ November 23, 2018

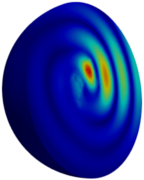

panorama of applications

- accurate prediction of coupled heat transfer at high temperatures
- heterogeneous materials offer a wide spectrum of thermo-mechanical and chemical properties
- design materials with optimum desired properties
- improve durability at extreme conditions
- going down the length scale for a deeper insight: micro-scales

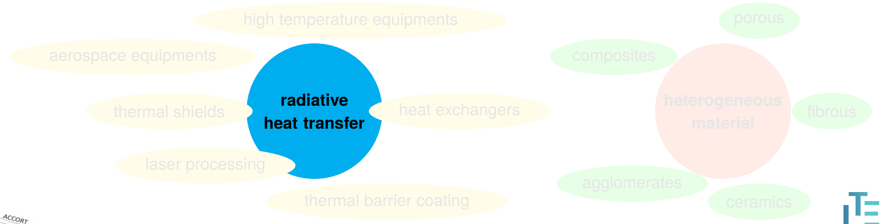

panorama of applications

- accurate prediction of coupled heat transfer at high temperatures
- heterogeneous materials offer a wide spectrum of thermo-mechanical and chemical properties
- design materials with optimum desired properties
- improve durability at extreme conditions
- going down the length scale for a deeper insight: micro-scales

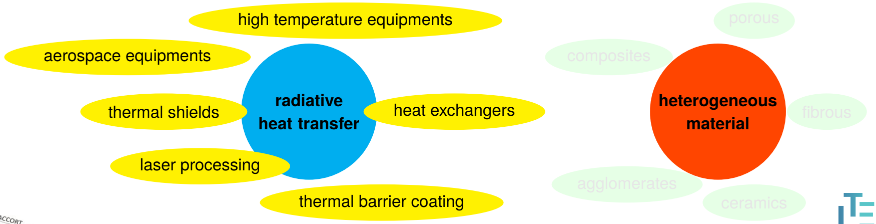

panorama of applications

- accurate prediction of coupled heat transfer at high temperatures
- heterogeneous materials offer a wide spectrum of thermo-mechanical and chemical properties
- design materials with optimum desired properties
- improve durability at extreme conditions
- going down the length scale for a deeper insight: micro-scales

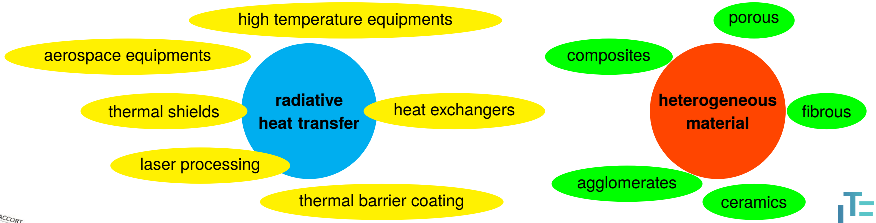

the setting

design cycle of an open-cell foam[1]

Texture

- 3D arrangement of scatterers in a host medium
- distribution of size, shape and orientation
- fine tune textural parameters
- tailor smart materials with optimal properties

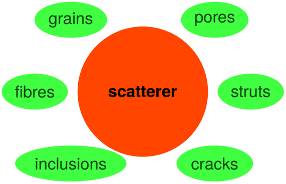

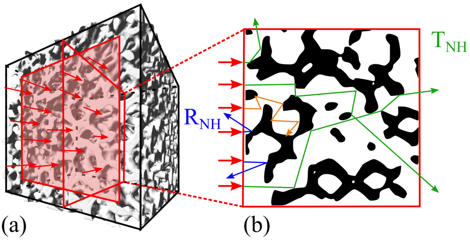

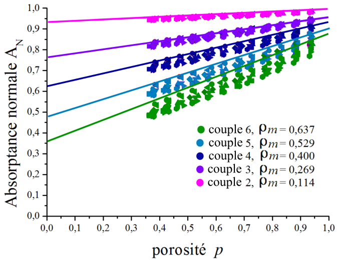

[1] S. Guévelou, B. Rousseau, G. Domingues, *et al.*, "Representative elementary volumes required to characterize the normal spectral emittance of silicon carbide foams used as volumetric solar absorbers," *International Journal of Heat and Mass Transfer*, 2016.

Texture

- 3D arrangement of scatterers in a host medium
- distribution of size, shape and orientation
- fine tune textural parameters
- tailor smart materials with optimal properties

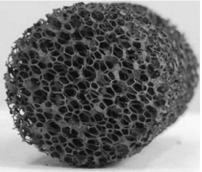

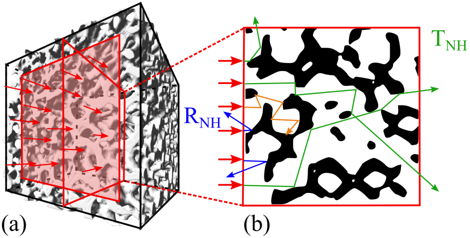

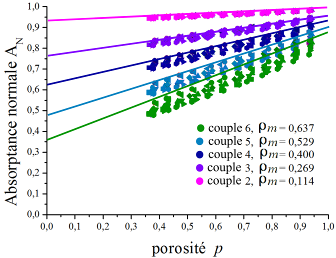

[1] S. Guévelou, B. Rousseau, G. Domingues, *et al.*, "Representative elementary volumes required to characterize the normal spectral emittance of silicon carbide foams used as volumetric solar absorbers," *International Journal of Heat and Mass Transfer*, 2016.

the setting

design cycle of an open-cell foam[1]

Texture

- 3D arrangement of scatterers in a host medium
- distribution of size, shape and orientation
- fine tune textural parameters
- tailor smart materials with optimal properties

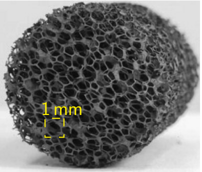

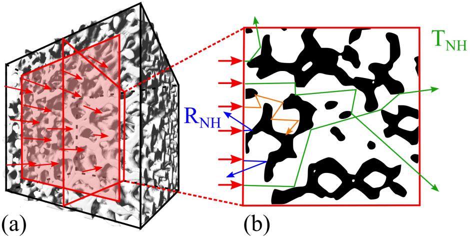

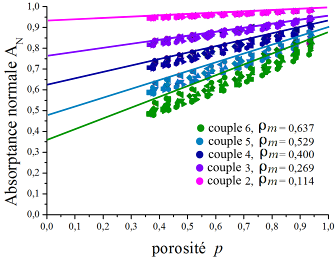

[1] S. Guévelou, B. Rousseau, G. Domingues, *et al.*, "Representative elementary volumes required to characterize the normal spectral emittance of silicon carbide foams used as volumetric solar absorbers," *International Journal of Heat and Mass Transfer*, 2016.

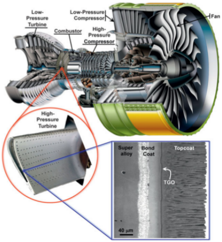

TBC in gas turbine[1]

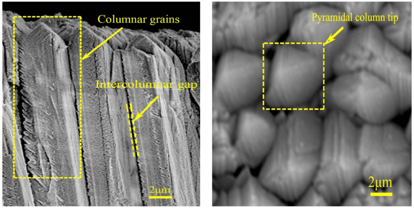

(a) Cross section of coating (b) top surface of coating

micro-structures in a thermal barrier coating[2]

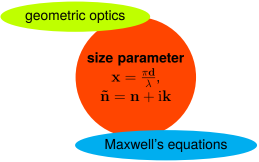

- today
  - challenging experiments
  - regular shapes
- attempts to reduce the gap of approximation made in terms of geometry

[1] D. R. Clarke, M. Oechsner, and N. P. Padture, “Thermal-barrier coatings for more efficient gas-turbine engines,” *MRS Bulletin*, vol. 37, no. 10, 891–898, 2012. DOI: 10.1557/mrs.2012.232.

[2] G. Yang and C. Zhao, “Infrared radiative properties of eb-pvd thermal barrier coatings,” *International Journal of Heat and Mass Transfer*, 2016.

the setting

world of Maxwell's equations

the setting

world of Maxwell's equations

Outline

Physical model

from macro to micro scale

radiative transfer equation

$$(\boldsymbol{s}\cdot\nabla)I(\boldsymbol{x},\boldsymbol{s})+\beta I(\boldsymbol{x},\boldsymbol{s})=\sigma_s\oint I(\boldsymbol{x},\boldsymbol{s}')\Phi(\boldsymbol{s},\boldsymbol{s}')\mathrm{d}\boldsymbol{s}' + \kappa I_b(\boldsymbol{x})$$

$\sigma_s \rightarrow$ scattering coefficient
$\beta \rightarrow$ extinction coefficient
$\Phi(\boldsymbol{s},\boldsymbol{s}') \rightarrow$ scattering phase function

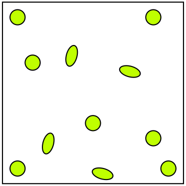

heterogeneous medium

- size parameter, $x = \frac{\pi d}{\lambda}$
- complex refractive index, $\tilde{n} = n + \mathrm{i}k$

$x\lvert\tilde{n}-1\rvert \ll 1$	Maxwell's
$x\lvert\tilde{n}-1\rvert \gg 1$	geometric optics

$\tilde{n}$, geometry

Maxwell's

$\bar{\sigma}_s$, $\bar{\beta}$, $\bar{\Phi}(\boldsymbol{s},\boldsymbol{s}')$

$$(\boldsymbol{s}\cdot\nabla)I(\boldsymbol{x},\boldsymbol{s})+\bar{\beta}I(\boldsymbol{x},\boldsymbol{s})=\bar{\sigma_s}\oint I(\boldsymbol{x},\boldsymbol{s}')\bar{\Phi}(\boldsymbol{s},\boldsymbol{s}')\mathrm{d}\boldsymbol{s}' + \bar{\kappa}I_b(\boldsymbol{x})$$

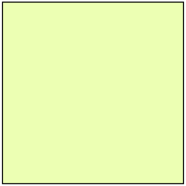

homogenized medium

$\bar{\sigma_s}$ $\rightarrow$ effective scattering coefficient
$\bar{\beta}$ $\rightarrow$ effective extinction coefficient
$\bar{\Phi}(\boldsymbol{s},\boldsymbol{s}')$ $\rightarrow$ effective scattering phase function

- size parameter, $x=\frac{\pi d}{\lambda}$
- complex refractive index, $\tilde{n}=n+\mathrm{i}k$

$x\lvert\tilde{n}-1\rvert \ll 1$	Maxwell's
$x\lvert\tilde{n}-1\rvert \gg 1$	geometric optics

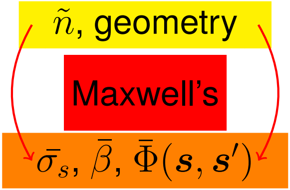

Mathematical model

electromagnetic scattering

frequency domain Maxwell's equations

$$\nabla \times \mathbf{H}(\boldsymbol{x},\omega) = \mathbf{J}(\boldsymbol{x},\omega) + \mathrm{i}\omega\epsilon_0\epsilon_r\mathbf{E}(\boldsymbol{x},\omega)$$
$$\nabla \times \mathbf{E}(\boldsymbol{x},\omega) = -\mathrm{i}\omega\mu_0\mu_r\mathbf{H}(\boldsymbol{x},\omega)$$
$$\nabla \cdot \mathbf{D}(\boldsymbol{x},\omega) = \rho_v$$
$$\nabla \cdot \mathbf{B}(\boldsymbol{x},\omega) = 0$$

$$\mathbf{D}(\boldsymbol{x},\omega) = \epsilon(\omega)\mathbf{E}(\boldsymbol{x},\omega)$$
$$\mathbf{B}(\boldsymbol{x},\omega) = \mu(\omega)\mathbf{H}(\boldsymbol{x},\omega)$$
$$\mathbf{J}(\boldsymbol{x},\omega) = \sigma(\omega)(\mathbf{E}(\boldsymbol{x},\omega) + \mathbf{E}_{\text{inc}}(\boldsymbol{x},\omega))$$

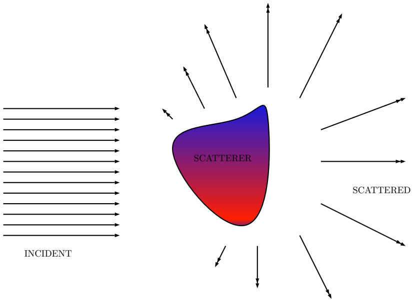

$\mathbf{H}(\boldsymbol{x},\omega)$	magnetic field intensity
$\mathbf{E}(\boldsymbol{x},\omega)$	electric field intensity
$\mathbf{J}(\boldsymbol{x},\omega)$	current density
$\mathbf{D}(\boldsymbol{x},\omega)$	electric displacement vector
$\mathbf{B}(\boldsymbol{x},\omega)$	magnetic flux density
ρ_v	volume charge density

$\epsilon = \epsilon_0\epsilon_r$	permittivity of medium
$\mu = \mu_0\mu_r$	permeability of medium
σ	electrical conductivity

$$\nabla \times \mathbf{H}(\boldsymbol{x},\omega) = \mathbf{J}(\boldsymbol{x},\omega) + \mathrm{i}\omega\epsilon_0\epsilon_r\mathbf{E}(\boldsymbol{x},\omega)$$
$$\nabla \times \mathbf{E}(\boldsymbol{x},\omega) = -\mathrm{i}\omega\mu_0\mu_r\mathbf{H}(\boldsymbol{x},\omega)$$
$$\nabla \cdot \mathbf{D}(\boldsymbol{x},\omega) = \rho_v$$
$$\nabla \cdot \mathbf{B}(\boldsymbol{x},\omega) = 0$$

$$\mathbf{D}(\boldsymbol{x},\omega) = \epsilon(\omega)\mathbf{E}(\boldsymbol{x},\omega)$$
$$\mathbf{B}(\boldsymbol{x},\omega) = \mu(\omega)\mathbf{H}(\boldsymbol{x},\omega)$$
$$\mathbf{J}(\boldsymbol{x},\omega) = \sigma(\omega)(\mathbf{E}(\boldsymbol{x},\omega) + \mathbf{E}_{\text{inc}}(\boldsymbol{x},\omega))$$

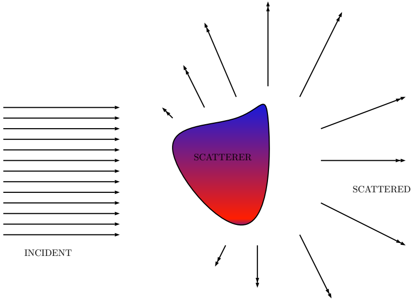

➤ vector wave equations

$$\nabla \times \frac{1}{\mu_r}\nabla \times \mathbf{E}(\boldsymbol{x},\omega) - k_0^2\epsilon_r\mathbf{E}(\boldsymbol{x},\omega) = 0$$

where for non-magnetic media,

$$\mu_r = 1,\ \epsilon_r = \epsilon' + \mathrm{i}\epsilon''$$
$$\epsilon' = n^2 - k^2,\ \ \epsilon'' = 2nk,\ k_0 = \omega\sqrt{\mu_0\epsilon_0}$$

Poynting vector, $\mathbf{S}$

$$\mathbf{S} = \frac{1}{2}\Re\left[\mathbf{E} \times \mathbf{H}^*\right]$$

$\Re$ - real part
* - complex conjugate

Incident energy, $\mathbf{S}_{\text{inc}}$

$$\mathbf{S}_{\text{inc}} = \frac{1}{2\eta}\left|\mathbf{E}_{\text{inc}}\right|^2\hat{\mathbf{k}}$$

$\eta = \sqrt{\frac{\mu}{\epsilon}}$: characteristic impedance
$\hat{\mathbf{k}}$: direction of incident wave

- with the solution of Maxwell's equations, $\mathbf{E}_{\text{sc}}$,

scattering, $\bar{\sigma_s}$

$$\mathrm{W}_{\text{sc}} = \frac{1}{2}\oint_{\Gamma_{\text{e}}} \Re\left[\mathbf{E}_{\text{sc}} \times \mathbf{H}_{\text{sc}}^*\right] \cdot \hat{\mathbf{n}}\,\mathrm{d}\boldsymbol{x}$$

$$\mathrm{C}_{\text{sc}} = \frac{|\mathrm{W}_{\text{sc}}|}{|\mathbf{S}_{\text{inc}}|},\ \bar{\sigma_s} = \sum_i \mathrm{C}_{\text{sc},i} N_{v,i}$$

extinction, $\bar{\beta}$

$$\mathrm{W}_{\text{ext}} = \frac{1}{2}\int_{\Gamma_{\text{e}}} \Re\left[\mathbf{E}_{\text{inc}} \times \mathbf{H}_{\text{sc}}^* + \mathbf{E}_{\text{sc}} \times \mathbf{H}_{\text{inc}}^*\right] \cdot \hat{\mathbf{n}}\,\mathrm{d}\boldsymbol{x}$$

$$\mathrm{C}_{\text{ext}} = \frac{|\mathrm{W}_{\text{ext}}|}{|\mathbf{S}_{\text{inc}}|},\ \bar{\beta} = \sum_i \mathrm{C}_{\text{exn},i} N_{v,i}$$

Γ_{e} - surface enclosing the scatterer(s) with unit normal $\hat{\mathbf{n}}$
$N_{v,i}$ - number density of scatterer i, $\left[\text{m}^{-3}\right]$

Poynting vector, $\mathbf{S}$

$$\mathbf{S} = \frac{1}{2}\Re\left[\mathbf{E} \times \mathbf{H}^*\right]$$

$\Re$ - real part
* - complex conjugate

Incident energy, $\mathbf{S}_{\text{inc}}$

$$\mathbf{S}_{\text{inc}} = \frac{1}{2\eta}\left|\mathbf{E}_{\text{inc}}\right|^2\hat{\mathbf{k}}$$

$\eta = \sqrt{\frac{\mu}{\epsilon}}$: characteristic impedance
$\hat{\mathbf{k}}$: direction of incident wave

- with the solution of Maxwell's equations, $\mathbf{E}_{\text{sc}}$,

asymmetry parameter, g

$$g = \frac{\int_{\Gamma_{\text{e}}} \cos\theta\, \mathbf{S}_{\text{sc}} \cdot \hat{\mathbf{n}}\, \mathrm{d}\boldsymbol{x}}{\int_{\Gamma_{\text{e}}} \mathbf{S}_{\text{sc}} \cdot \hat{\mathbf{n}}\, \mathrm{d}\boldsymbol{x}}$$

$$\mathbf{S}_{\text{sc}} = \frac{1}{2}\Re\left[\mathbf{E}_{\text{sc}} \times \mathbf{H}^*_{\text{sc}}\right]$$

$\cos\theta = \hat{\mathbf{n}} \cdot \hat{\mathbf{k}}$ is directional cosine between unit normal vector $\hat{\mathbf{n}}$ and incident plane wave direction $\hat{\mathbf{k}}$

Numerical model

edge degrees of freedom

- ensure tangential continuity $\mathbf{n} \times \mathbf{E}$ of the field vector $\mathbf{E}$
- avoid spurious solutions, as with nodal elements

for a finite element $\mathrm{T} \in \hat{\mathcal{T}}$

$$\int_{\mathrm{T}} (\nabla \times \mathbf{E}) \cdot \hat{\mathbf{n}}_e \mathrm{d}\boldsymbol{x} = \int_{\partial \mathrm{T}} \mathbf{E}.\hat{\tau} \mathrm{d}\boldsymbol{x}$$

$\hat{\mathcal{T}}$ - triangulation of the domain Ω truncated by Γ
$\hat{\mathbf{n}}_e$ - unit normal vector of T
$\hat{\tau}$ - unit tangent vector to edge $\partial \mathrm{T}$

vector functional space[3] for Maxwell's equation

$$\mathcal{H}(\text{curl}, \Omega) = \{\mathbf{E} \in \mathrm{L}^2(\Omega)^n \mid \nabla \times \mathbf{E} \in \mathrm{L}^2(\Omega)^n\},\ n = 2, 3$$

[3] A. Bossavit, "A rationale for 'edge-elements' in 3-d fields computations," *IEEE Transactions on Magnetics*, 1988.

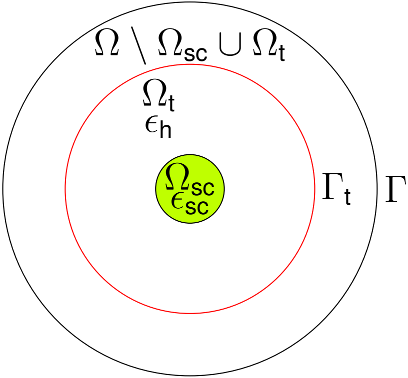

$$\nabla \times \nabla \times \mathbf{E}_{\text{sc}} - k_0^2 \epsilon \mathbf{E}_{\text{sc}} = 0, \text{ in } \Omega \setminus \Omega_{\text{sc}} \cup \Omega_{\text{t}}$$

$$\nabla \times \nabla \times \mathbf{E} - k_0^2 \epsilon \mathbf{E} = \nabla \times \nabla \times \mathbf{E}_{\text{inc}} - k_0^2 \epsilon_h \mathbf{E}_{\text{inc}}, \text{ in } \Omega_{\text{sc}} \cup \Omega_{\text{t}}$$

$$\mathbf{E} = \mathbf{E}_{\text{sc}} + \mathbf{E}_{\text{inc}}$$

with first-order absorbing boundary condition for $\mathbf{E}_{\text{sc}}$,

$$\mathbf{n} \times \nabla \times \mathbf{E}_{\text{sc}} + \mathrm{i} k_0 \mathbf{n} \times \mathbf{n} \times \mathbf{E}_{\text{sc}} = 0, \text{ on } \Gamma$$

ϵ_{h} - permittivitty of the host medium

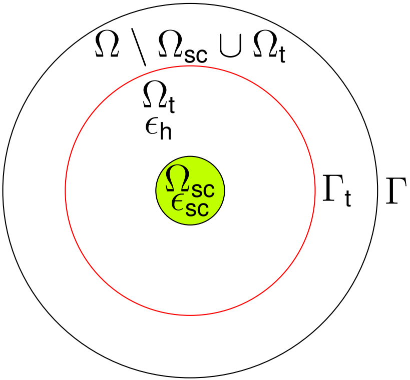

find $\mathbf{E}_{sc} \in \mathcal{H}(\text{curl}, \Omega)$ such that,

$$\int_{\Omega} \left[(\nabla \times \mathbf{V}^*) \cdot (\nabla \times \mathbf{E}_{sc}) - k_0^2 \epsilon \mathbf{V}^* \cdot \mathbf{E}_{sc} \right] \mathrm{d}\boldsymbol{x} - \mathrm{i} k_0 \int_{\Gamma} (\mathbf{n} \times \mathbf{V}^*) \cdot (\mathbf{n} \times \mathbf{E}_{sc}) \, \mathrm{d}\boldsymbol{x}$$

$$= k_0^2 \int_{\Omega_t \cup \Omega_{sc}} (\epsilon_{sc} - \epsilon_h) \, \mathbf{V}^* \cdot \mathbf{E}_{inc} \, \mathrm{d}\boldsymbol{x}, \; \forall \, \mathbf{V} \in \mathcal{H}_0(\text{curl}, \Omega)$$

$$(\mathbf{u},\mathbf{v})_{\mathrm{L}^2(\Omega)} = \int_\Omega \mathbf{v}^* \cdot \mathbf{u}\,\mathrm{d}\boldsymbol{x} \quad \mathbf{u},\mathbf{v} \in \mathbb{C},$$

$$\mathbf{E}_{\text{sc}} = \sum_{i=1}^{n_{\text{dof}}} \alpha_i \boldsymbol{\Psi}_i, \qquad \mathbf{V} = \Psi_j,\ \forall j = 1 \to n_{\text{dof}}$$

n_{dof} - number of degrees of freedom

$$[\mathbf{C}+\mathbf{M}+\mathbf{B}][\mathbf{E}_{\text{sc}}] = [\mathbf{L}]$$

$$[\mathbf{C}]_{ij} = (\nabla\times\boldsymbol{\Psi}_j, \nabla\times\boldsymbol{\Psi}_i)_\Omega \qquad [\mathbf{M}]_{ij} = -k_0^2(\boldsymbol{\Psi}_j, \epsilon\boldsymbol{\Psi}_i)_\Omega$$

$$[\mathbf{B}]_{ij} = -\mathrm{i}k_0(\mathbf{n}\times\boldsymbol{\Psi}_j, \mathbf{n}\times\boldsymbol{\Psi}_i)_\Gamma \qquad [\mathbf{L}]_j = k_0^2(\boldsymbol{\Psi}_\mathbf{j}, (\epsilon_{\text{sc}}-\epsilon_{\text{h}})\mathbf{E}_{\text{inc}})_{\Omega_{\text{t}}\cup\Omega_{\text{sc}}}$$

demands linear algebra expertise

- ill-conditioned
- edge elements, huge number of unknowns
- iterative methods

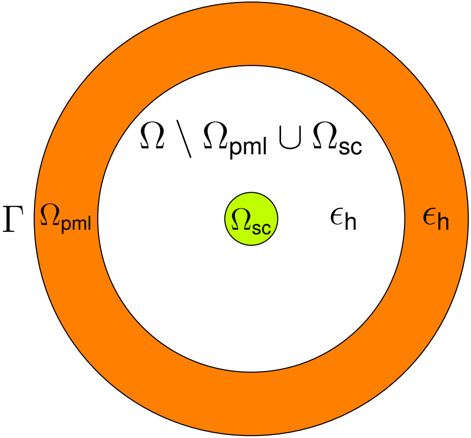

an absorbing layer

- prevent artificial reflections[4]
- not a boundary condition, can be augmented with ABC

[4] J.-P. Berenger, "A perfectly matched layer for the absorption of electromagnetic waves," *Journal of Computational Physics*, 1994.

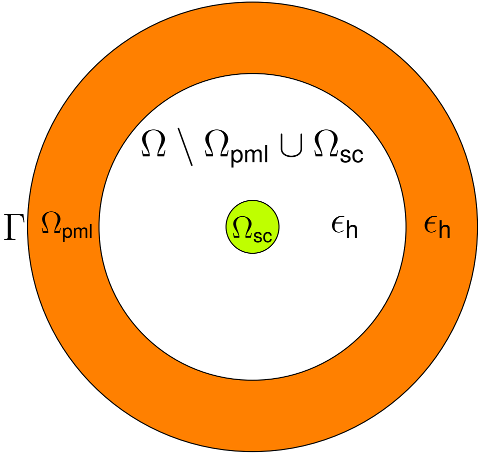

$$\bar{\bar{M}} = \begin{bmatrix} \gamma_r(\boldsymbol{x}) & 0 \\ 0 & \frac{1}{\gamma_r(\boldsymbol{x})} \end{bmatrix},$$

$$N = \gamma_r(\boldsymbol{x})\gamma_r(\boldsymbol{x})$$

$$\forall \boldsymbol{x} \in \Omega^n,\ n = 2$$

δ_{pml} - thickness of Ω_{pml}

$$\epsilon^p = N\epsilon$$

$$\mu^p = \bar{\bar{M}}\mu$$

$$\gamma_r(\boldsymbol{x}) = 1 + \mathrm{i}\sigma_r(\boldsymbol{x})$$

$$\sigma_r(\boldsymbol{x}) = \begin{cases} s_r\left(\sin\frac{\pi(|\boldsymbol{x}-\boldsymbol{x}_0|-r_d)}{2\delta_{\text{pml}}}\right)^{\alpha}, & \text{if } |\boldsymbol{x}-\boldsymbol{x}_0| - r_d > 0 \\ 0, & \text{if } |\boldsymbol{x}-\boldsymbol{x}_0| - r_d \leq 0 \end{cases},\ \forall \boldsymbol{x} \in \Omega^n,\ n = 2, 3$$

r_d - distance from center $\boldsymbol{x}_0$ to Ω_{pml}

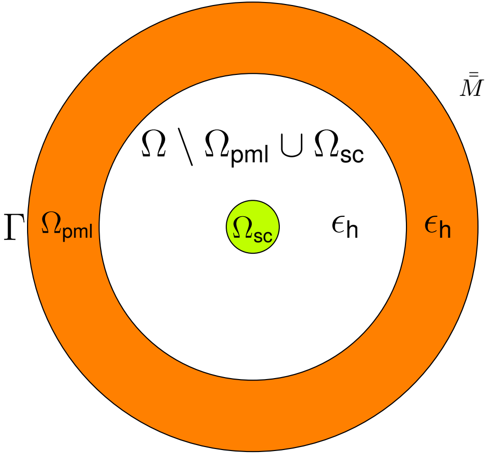

$$\bar{\bar{M}} = \begin{bmatrix} \gamma_r(\boldsymbol{x}) & 0 & 0 \\ 0 & \gamma_r(\boldsymbol{x}) & 0 \\ 0 & 0 & \frac{1}{\gamma_r(\boldsymbol{x})} \end{bmatrix}$$

$$N = \gamma_r(\boldsymbol{x})\gamma_r(\boldsymbol{x})\gamma_r(\boldsymbol{x}),$$

$$\forall \boldsymbol{x} \in \Omega^n, \ n = 3$$

δ_{pml} - thickness of Ω_{pml}

$$\epsilon^p = N\epsilon$$
$$\mu^p = \bar{\bar{M}}\mu$$

$$\gamma_r(\boldsymbol{x}) = 1 + \mathrm{i}\sigma_r(\boldsymbol{x})$$

$$\sigma_r(\boldsymbol{x}) = \begin{cases} s_r\left(\sin\frac{\pi(|\boldsymbol{x}-\boldsymbol{x}_0|-r_d)}{2\delta_{\text{pml}}}\right)^{\alpha}, & \text{if } |\boldsymbol{x}-\boldsymbol{x}_0| - r_d > 0 \\ 0, & \text{if } |\boldsymbol{x}-\boldsymbol{x}_0| - r_d \leq 0 \end{cases}, \ \forall \boldsymbol{x} \in \Omega^n, \ n = 2, 3$$

r_d - distance from center $\boldsymbol{x}_0$ to Ω_{pml}

Numerical experiments

finite element package	FreeFem++[4]
mesh generation	gmsh[5]
solution strategy	direct iterative
iterative solver packages	PETSc[6], hpddm[7]
domain truncation	ABC, PML
$\mathbf{E}_{\text{inc}}$	$[0,0,e^{\mathrm{i}k_0 x}]$

[4] F. Hecht, "New development in freefem++," *J. Numer. Math.*, vol. 20, no. 3-4, 2012.

[5] C. Geuzaine and J.-F. Remacle, "Gmsh: A 3-d finite element mesh generator with built-in pre- and post-processing facilities," *International Journal for Numerical Methods in Engineering*, 2009.

[6] S. Balay, W. D. Gropp, L. C. McInnes, *et al.*, "Efficient management of parallelism in object oriented numerical software libraries," in *Modern Software Tools in Scientific Computing*, Birkhäuser Press, 1997.

[7] P. Jolivet, F. Hecht, F. Nataf, *et al.*, "Scalable domain decomposition preconditioners for heterogeneous elliptic problems," in *Proceedings of the International Conference on High Performance Computing, Networking, Storage and Analysis*, ACM, 2013.

infinite regular cylinder

Validation, 2D (TE mode)

parameters

λ	3 µm - 24 µm
$\tilde{n}$	silica
d	7 µm
$\frac{\pi d}{\lambda}$	0.92 - 7.33

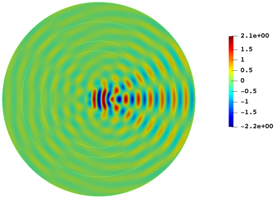

$\Re(E_{\text{sc}}) \in \mathcal{H}^1(\Omega)$

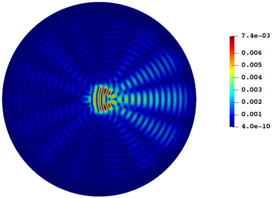

$\Re(\mathbf{H}_{\text{sc}}) \in \mathcal{H}(\text{curl}, \Omega)$

Figure: $\lambda = 3$ µm

scattering efficiency, $\frac{C_{\text{sc}}}{d}$

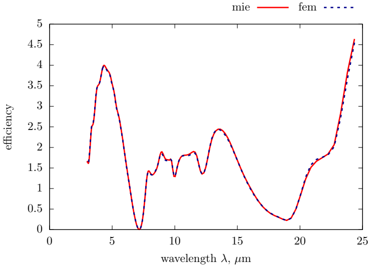

extinction efficiency, $\frac{C_{\text{exn}}}{d}$

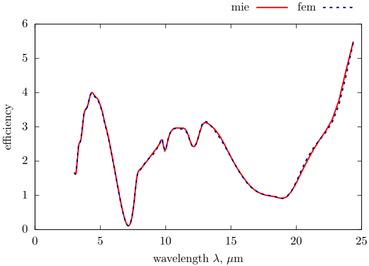

parameters

λ	3 µm - 24 µm
$\tilde{n}$	silica
d	7 µm
$\frac{\pi d}{\lambda}$	0.92 - 7.33

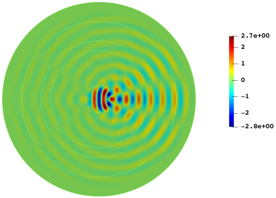

$\Re(H_{\text{sc}}) \in \mathcal{H}^1(\Omega)$

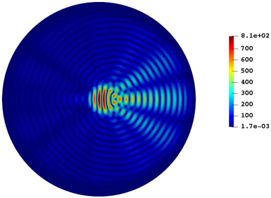

$\Re(\mathbf{E}_{\text{sc}}) \in \mathcal{H}(\text{curl}, \Omega)$

Figure: λ =3 µm

scattering efficiency, $\frac{C_{\text{sc}}}{d}$

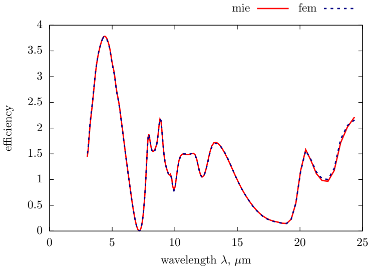

extinction efficiency, $\frac{C_{\text{exn}}}{d}$

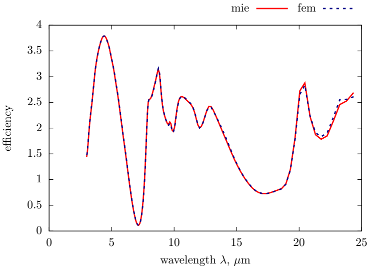

parameters

$\tilde{n}$	silica
λ	3 µm - 24 µm
$\bar{d}$	2.30 µm

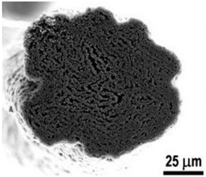

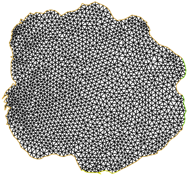

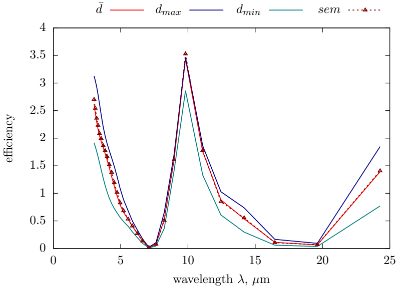

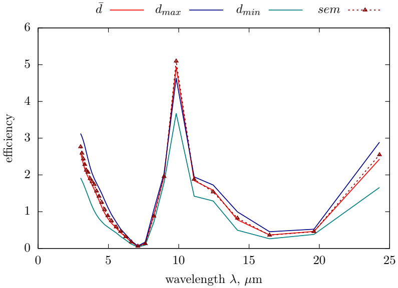

[8] M. D. Lima, S. Fang, X. Lepró, *et al.*, “Biscrolling nanotube sheets and functional guests into yarns,” *Science*, 2011.

parameters

$\tilde{n}$	silica
λ	3 µm - 24 µm
$\bar{d}$	2.30 µm

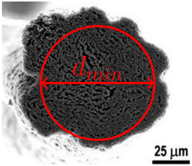

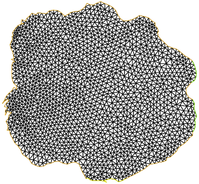

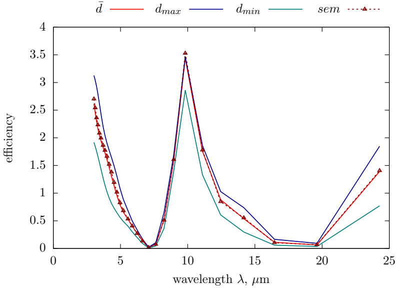

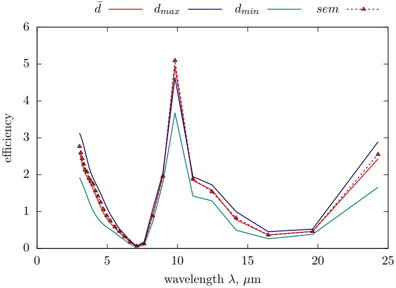

[8] M. D. Lima, S. Fang, X. Lepró, *et al.*, "Biscrolling nanotube sheets and functional guests into yarns," *Science*, 2011.

infinite complex cylinder

sem[8] to fem (TE mode)

parameters

$\tilde{n}$	silica
λ	3 µm - 24 µm
$\bar{d}$	7 µm

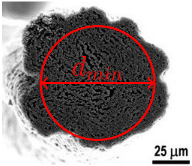

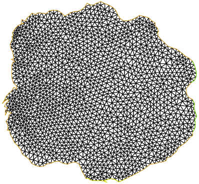

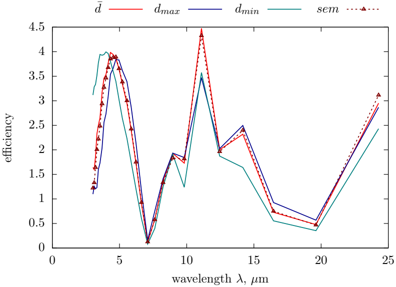

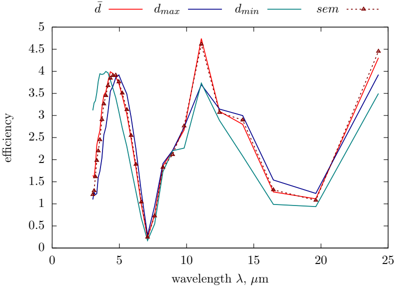

[8] M. D. Lima, S. Fang, X. Lepró, *et al.*, "Biscrolling nanotube sheets and functional guests into yarns," *Science*, 2011.

parameters

$\tilde{n}$	silica
λ	3 µm - 24 µm
$\bar{d}$	21 µm

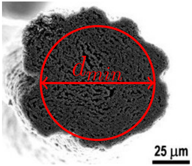

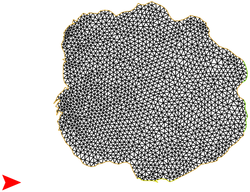

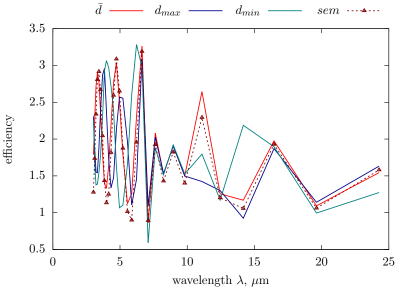

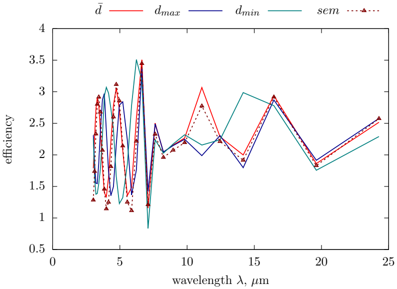

[8] M. D. Lima, S. Fang, X. Lepró, *et al.*, "Biscrolling nanotube sheets and functional guests into yarns," *Science*, 2011.

parameters

$\tilde{n}$	silica
λ	3 µm - 24 µm
$\bar{d}$	2.30 µm

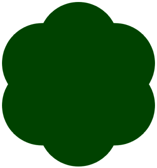

Figure: Ω_{sc}

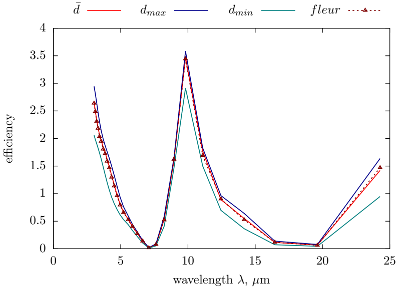

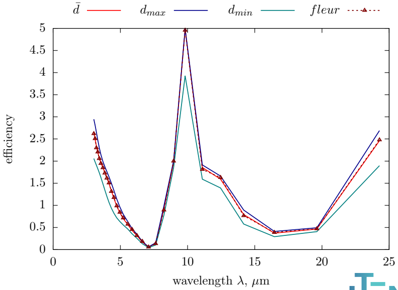

infinite complex cylinder

la fleur (TE mode)

parameters

$\tilde{n}$	silica
λ	3 µm - 24 µm
$\bar{d}$	7 µm

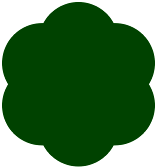

Figure: Ω_{sc}

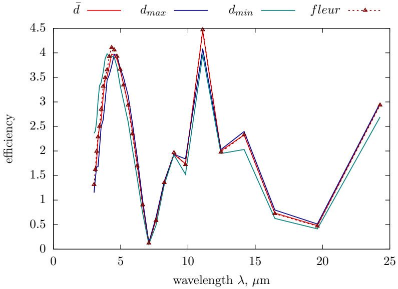

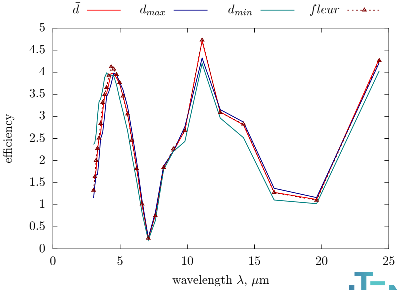

parameters

$\tilde{n}$	silica
λ	3 µm - 24 µm
$\bar{d}$	21 µm

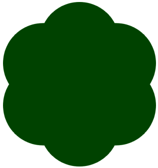

Figure: Ω_{sc}

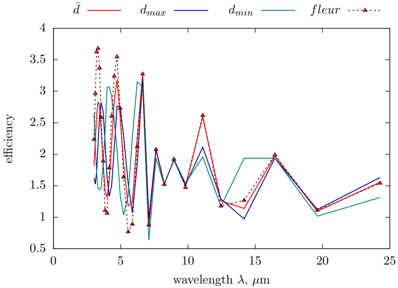

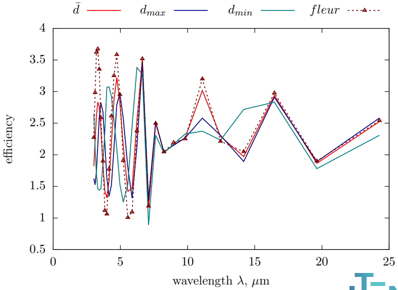

parameters

$\tilde{n}$	silica
λ	3 µm - 24 µm
$\bar{d}$	63 µm

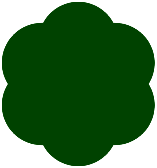

Figure: Ω_{sc}

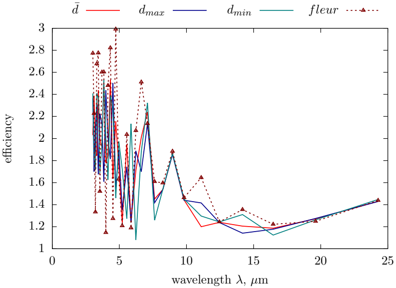

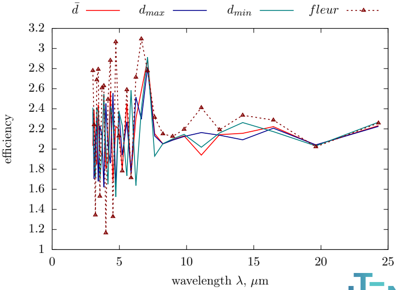

- number of processes[9]: 400

$\tilde{n}$	$1.34548 + 0.00407i$
λ	6 µm
d	6 µm
tetrahedra	$\approx$ 25 million

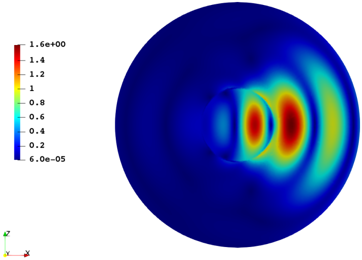

Figure: $\Re(\mathbf{E}_{sc}) \in \mathcal{H}(\text{curl}, \Omega)$at $z = 0$

challenges

- accuracy comes at a cost
- ill-conditioned, not robust
- needs preconditioning

	mie	fem	% error
C_{exn}	2.095089	2.09998	0.2334
C_{sc}	2.042769	2.04942	0.3256
C_{abs}	0.052320	0.0505623	3.36
g	0.791642	0.818101	3.3423

[9]CCIPL - Le centre de calcul intensif des Pays de la Loire

some 3D computations

single kelvin cell

- number of processes[9]: 400

$\tilde{n}$	$1.34548 + 0.00407i$
λ	5 µm
diameter of pore	5 µm
porosity, ϕ	$60 \; - \; 90 \; \%$
tetrahedra	$\approx$ 20 million

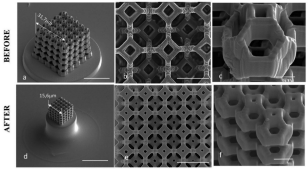

application in nanofabrication[10]

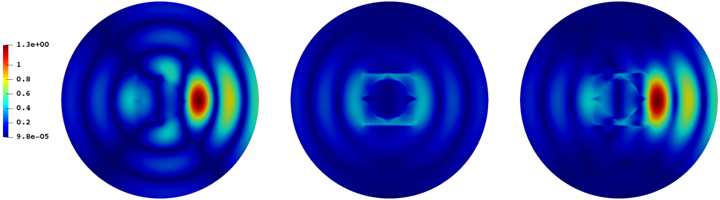

Figure: $\Re(\mathbf{E}_{\text{sc}}) \in \mathcal{H}(\text{curl}, \Omega)$ at $z = 0$, $x = 0$, $y = 0$ for $\phi = 60\ \%$

[9] CCIPL - Le centre de calcul intensif des Pays de la Loire

[10] L. Brigo, J. E. M. Schmidt, A. Gandin, *et al.*, "3d nanofabrication of sioc ceramic structures," *Advanced Science*,

- number of processes[9]: 400

$\tilde{n}$	$1.34548 + 0.00407\mathrm{i}$
λ	5 µm
diameter of pore	5 µm
porosity, ϕ	$60 \;-\; 90\ \%$
tetrahedra	$\approx$ 20 million

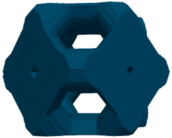

$\phi = 60\ \%$

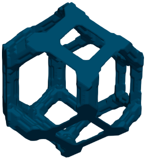

$\phi = 90\ \%$

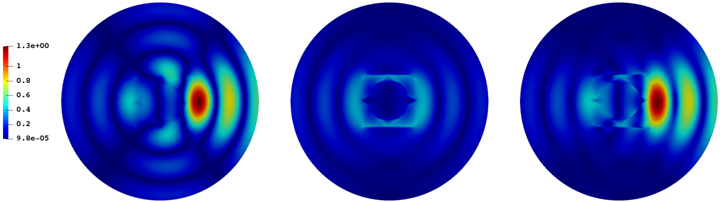

Figure: $\Re(\mathbf{E}_{\text{sc}}) \in \mathcal{H}(\text{curl}, \Omega)$ at $z = 0$, $x = 0$, $y = 0$ for $\phi = 60\ \%$

[9]CCIPL - Le centre de calcul intensif des Pays de la Loire

- number of processes[9]: 400

$\tilde{n}$	$1.34548 + 0.00407i$
λ	5 µm
diameter of pore	5 µm
porosity, ϕ	$60 \ - \ 90\ \%$
tetrahedra	≈ 20 million

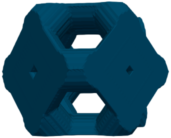

$\phi = 60\ \%$

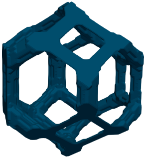

$\phi = 90\ \%$

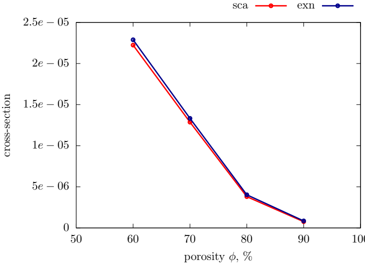

C_{sc}, C_{exn} vs ϕ

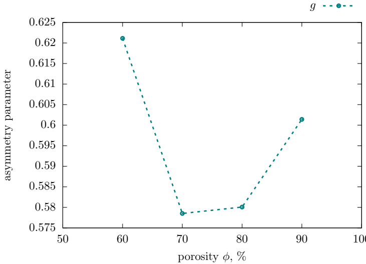

g vs ϕ

[9] CCIPL - Le centre de calcul intensif des Pays de la Loire

Conclusion

summary

- finite element tool developed, validated in 2D and 3D
- iterative solving based on domain-decomposition
- influence of morphology on infinite cylinders studied briefly
- single kelvin cell has been studied for ϕ: $60 - 90\,\%$

challenges

- expensive 3D computations
- ill-conditioning, dense linear system: edge elements
- efficient mesh truncation

preconditioning

- optimized Schwarz methods with a coarse space[10]
- strive for a robust solving strategy

[10] M. Bonazzoli, V. Dolean, I. Graham, *et al.*, "A two-level domain-decomposition preconditioner for the time-harmonic maxwell's equations," *Hal archives*, 2018.

summary

- finite element tool developed, validated in 2D and 3D
- iterative solving based on domain-decomposition
- influence of morphology on infinite cylinders studied briefly
- single kelvin cell has been studied for ϕ: $60 - 90\,\%$

challenges

- expensive 3D computations
- ill-conditioning, dense linear system: edge elements
- efficient mesh truncation

towards better understanding of radiative behaviour

- explore closely **independent-dependent scattering** regimes
- identify the **limit** of geometric optics approximation: material design
- coupling with other numerical methods

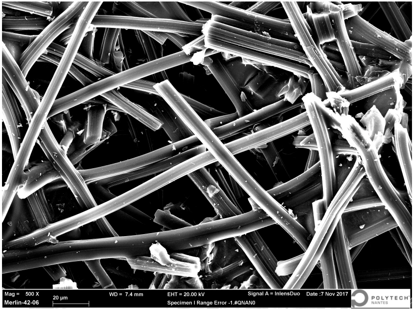

(a) SEM image (µm)

(b) X-ray tomography image (mm)

Figure: closely packed fibers of carbon felt

prospective heterogeneous medium

- in (b) - number of voxels: $400 \times 400 \times 400$, voxel edge length: 1.65 µm
- insulation of high temperature furnace[10]
- linear system resulting from (b) will be difficult to handle

[10] co-thesis: Atin Kumar

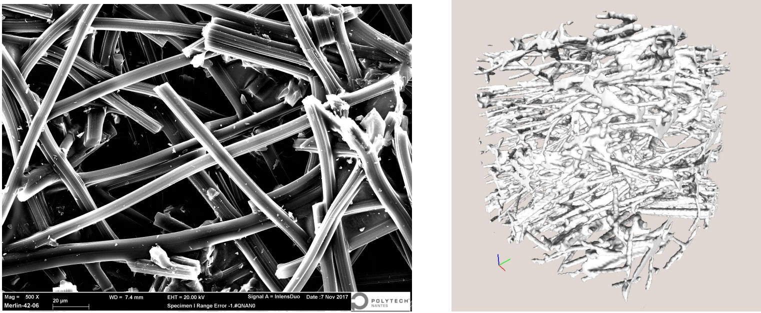

(a) SEM image (µm) (b) X-ray tomography image (mm)

Figure: closely packed fibers of carbon felt

more accurate input to the radiative transfer equation

- strive for efficient treatment of individual fibers, as in (a)
- homogenize the heterogeneous medium